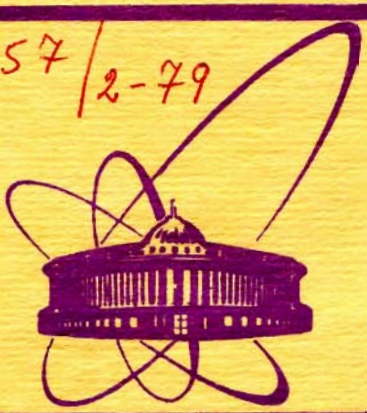

сообщения
объединенного
института
ядерных
исследований
дубна

E2 - 12686

R.A.Eramzhyan, M.Gmitro, H.R.Kissener

GIANT M2 AND TRANSVERSAL E1 RESONANCES IN LIGHT NUCLEI

1979

E2 - 12686

R.A.Eramzhyan, M.Gmitro, H.R.Kissener *

GIANT M2 AND TRANSVERSAL E1 RESONANCES IN LIGHT NUCLEI

* Zentralinstitut für Kernforschung, Rossendorf, DDR.

Эрамжян Р.А., Гмитро М., Киссенер Х.Р.

E2 - 12686

Гигантские М2 и Е1t резонансы в легких ядрах

В рамках модели оболочек проведен расчет сечения неупругого рассеяния электронов назад при энергии E_e = 70 МэВ на ядрах p -оболочки. Проведено сравнение этой реакции с реакцией радиационного захвата пионов. Рассмотрены ядра ^{7}Li, ^{9}Be, ^{11}Be, ^{13}C, ^{14}C, ^{14}N и ^{16}O. Показано, что одни и те же переходы формируют $T_>$ ветвь М2 резонанса в реакции (e,e′) и основной максимум в спектре возбуждения ядра в реакции (π^-,γ). Выявлены основные закономерности возбуждения М2-резонанса в ядрах p-оболочки. Предсказано конфигурационное и изоспиновое расщепление этого резонанса.

Работа выполнена в Лаборатории теоретической физики ОИЯИ.

Сообщение Объединенного института ядерных исследований. Дубна 1979

Eramzhyan R.A., Gmitro M., Kissener H.R.

E2 - 12686

Giant M2 and Transversal E1 Resonances in Light Nuclei

The cross section for inelastic backward electron scattering on 1p shell nuclei at incident energy E_e = 70 MeV is calculated in the shell model. Comparison is made with radiative pion capture and muon capture. It is shown that the $T_>$ branch of the M2 resonance in (e,e′) and the main maxima in the (π^-,γ) response function are formed by identical partial transitions. We consider the basic feature of the M2 resonance excitation in 1p shell nuclei and predict configurational and isospin splitting of this mode.

The investigation has been performed at the Laboratory of Theoretical Physics, JINR.

Communication of the Joint Institute for Nuclear Research. Dubna 1979

1. Introduction

Systematic studies of radiative pion capture by light nuclei show the formation of nuclear collective states [1,2], similar to the case of photonuclear reactions, muon capture and other low-q transfer reactions at intermediate energies. In contrast to the photo giant resonance, the main contribution of the (π^-, γ) yield is due to the (axial-vector) spin-multipole transitions. Earlier a clear evidence was found for the analogy between the well-resolved partial transitions at the high-energy end of the hard γ-ray spectrum of (π^-, γ) and the M1 resonance in 1p shell nuclei [3,4].

The analogy between the strong partial transitions in these reactions is supposed to extend also to higher magnetic multipoles. At present, however, M2 resonances have been established in electroexcitation only for few spherical nuclei [5-8]. Theoretical work on M2 electroexcitation was performed systematically for medium and heavy nuclei [9,10] and for a few light nuclei, e.g., ^{12}C and ^{16}O (ref. [11]), ^{13}C and ^{14}C (ref. [12]). Similarly to the case of M1 resonance [5], one expects the concentration of M2

strength to decrease gradually from the lighter to heavier nuclei and hence believes the light nuclei to be particularly prospective for the experimental investigation of this mode.

The purpose of this paper is to demonstrate that the main maximum in the (π^-, γ) response curve for the 1p shell nuclei corresponds to the same transitions which form the M2, $T_>$ resonance in electroexcitation. For this reason we calculate the inelastic electron scattering cross sections at backward angles and choose the same momentum transfer as is realized in the radiative pion capture (incident energy E_e = 70 MeV). Under these conditions M1 and transversal electric dipole (E1t) and possibly electric quadrupole transitions also contribute to the (e,e') cross section, the latter two modes should be absent in the (π^-, γ) process as follows from the structure of the elementary amplitudes. Since M1 resonances in (e , e'), (π^-, γ) and (μ^- , ν_μ) were already reviewed elsewhere [1,3,13], we do not include them here.

2. Basic formulae

Disregarding M1 terms, backward electroexcitation on light nuclei at momentum transfer $q \approx m_\pi$ is described essentially by M2 and E1t multipoles,

$$\left(\frac{d\sigma}{d\Omega}\right)_{180^\circ} = \frac{\pi\alpha^2}{E_e^2}\,\frac{1}{2J_i+1}\left\{ \left|\langle J_f \| T_1^{el}(q) \| J_i\rangle\right|^2 + \left|\langle J_f \| T_2^{mag}(q) \| J_i\rangle\right|^2 \right\}, \qquad (1)$$

where

$$T_2^{mag}(q) = i\,\frac{q}{2M}\left\{ -2Q_{122}\left(\frac{\vec{\nabla}}{q}\right)\frac{1+\tau_3}{2} + \left[\sqrt{\tfrac{3}{5}}\,Q_{112}(\vec{\sigma}) - \sqrt{\tfrac{2}{5}}\,Q_{132}(\vec{\sigma})\right]\left[\frac{\mu_p+\mu_n}{2} + \frac{\mu_p-\mu_n}{2}\tau_3\right]\right\}, \qquad (2)$$

$$T_1^{el}(q) = \frac{q}{2M}\left\{ 2\,\frac{1+\tau_3}{2}\left[\sqrt{\tfrac{2}{3}}\,Q_{101}\left(\frac{\vec{\nabla}}{q}\right) - \sqrt{\tfrac{1}{3}}\,Q_{121}\left(\frac{\vec{\nabla}}{q}\right)\right] + Q_{111}(\vec{\sigma})\left[\frac{\mu_p+\mu_n}{2} + \frac{\mu_p-\mu_n}{2}\tau_3\right]\right\}, \qquad (3)$$

and

$$Q_{1wJM}(\vec{a}) = j_w(qr)\left[\vec{a} \times Y_w(\hat{r})\right]_{JM}, \qquad (4)$$

E_e being the incident energy.

The nuclear radiative-pion-capture amplitude is described by a set of operators [1] which after performing the multipole decomposition can be written as follows

$$T_{JM}(\vec{\sigma}) = \sum_{w} \left[\vec{\sigma} \times Y_w(\hat{r})\right]_{JM} F(r; w, J), \qquad (5)$$

the function $F(r; w, J)$ containing the pion radial wave function in mesoatom, the spherical Bessel function from the expansion of the photon wave, and some vector coupling coefficients. The yield R_γ of γ-quanta (which is usually measured) is expressed by matrix elements of the operators (5). For light nuclei, the first term in (5), $w=0$, corresponds to transitions forming the M1 resonance. The main maximum in the γ-spectrum is connected with the $[\sigma \times Y_1]_J$- terms [1]. The low-energy part of the primary γ-spectrum where the resonance structure practically disappears is due to the $[\sigma \times Y_2]_{J^+}$ operators. In the 1p shell nuclei these latter transitions do not show collectivity [14], their numerous contributions rather add up to a smooth curve, both in the excitation and in the neutron emission spectra [15]. The contribution of transitions with $w>2$ is negligible for light nuclei.

In muon capture the main contribution to the total capture rate Λ_μ is due to dipole (vector current) and $w=0$ and 1 spin-multipole (axial-vector current) excitation. For $J^\pi=0^+$ target nuclei the transitions to states with $J_f^\pi = 1^-$ and 2^- essentially account for the total rate. In the $J_f^\pi=1^-$ branch both vector and axial-vector operators are involved, whereas the $0^+ \to 2^-$ transitions are mainly governed by the axial-vector terms (4) with $\vec{\alpha}=\vec{\sigma}$ and $w=1$, see ref. [14].

The spin-dipole part of operator (5) that is mainly responsible for the (π,γ) reaction resembles closely the dominating term $Q_{112}(\sigma)$ of the T_2^{mag} operator (2). When taken in the long-wavelength limit T_2^{mag} describes the M2 photo absorption transitions. At low q-values radial parts of these operators are also similar to each other; e.g., the F factor of eq. (5) essentially contains the same spherical Bessel functions as (2), which are only slightly weighted by the (slowly varying) pion radial wave function.

Since in addition we consider the creation of the collective nuclear states to be universal response of the atomic nuclei to the excitation agent independently of its particular nature (photo-excitation, (e,e') scattering, lepton-or meson-induced processes) the resonances created in the (π^-,γ) and (μ^-,ν_μ) processes should be formed by the same transitions as these in the case of the M2 transitions in the (e,e') reaction. In the present work the excitation spectra for the (e,e') reaction on ^{16}O, ^{14}N, ^{14}C, ^{13}C, ^{11}B, ^{9}Be and ^{7}Li are to be discussed in comparison with the earlier results [3,4,13] for the radiative pion capture spectra and muon capture rates. The nuclear system with A=16 has been considered [14] in the np-nh $(n=0,1,2)$ shell model; we take the nuclear wave function for the A=14,13,11,9,7 nuclei from ref.[4]. They were calculated by the standard diagonalization of a residual force within complete subspaces of $1\hbar\omega$ non-spurious configurations.

3. Resonances in A=16 nuclear system

The ^{16}O response function for several reactions is shown in fig. 1 as follows:

(i) backward e^- scattering, the M2 transitions are singled out.

(ii) spin-dipole $(w=1)$ branch of (π^-,γ) reaction (the total spectrum is shown in ref.[15]).

(iii) muon capture rate, and

(iv) backward e^- scattering, including both M2 and E1t transitions

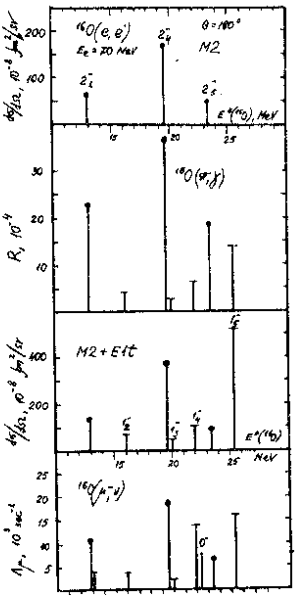

Fig. 1. A=16 nuclear excitation spectra in reactions (e,e'), (π^-,γ) and (μ^-,ν_μ).

Table 1. Single particle matrix elements of operators T_1^{el} and T_2^{mag}, eqs. (2) and (3) calculated in the harmonic oscillator basis with b = 1.67 fm.

		T_1^{el} (q)		T_2^{mag} (q)	
		$p_{3/2}$	$p_{1/2}$	$p_{3/2}$	$p_{1/2}$
$d_{5/2}$	a)	-0.0677	-	0.0032	-0.0028
	b)	-0.0045	-	0.0625	-0.0549
$s_{1/2}$	a)	-0.0346	-0.0221	0.0019	-
	b)	-0.0524	+0.0040	0.0335	-
$d_{3/2}$	a)	0.0265	-0.0540	0.0009	-0.0003
	b)	0.0788	-0.0725	0.0203	-0.0028

a) q = 20 MeV/c

b) q = 100 MeV/c

The M2 resonance is essentially connected with the $p_{3/2} \rightarrow d_{5/2}$ transition, see table 1. The M2 strength is concentrated on the $J^\pi = 2_4^-$ (19 MeV) level (the lower index indicates the item number of a state). Two other peaks at $E^* = 12$ MeV and 22 MeV are excited with lesser intensity. Similar relations can be seen in the (π^-, γ) reaction too: the intensity of excitation of the 2^- levels in ^{16}N repeats the corresponding values of the (e, e') reaction for T=1 levels in ^{16}O. Therefore, these calculations demonstrate that the transitions in the (π^-, γ) reactions show up collectivity in very much the same manner, as in M2 transitions. Indeed, due to the difference in the isospin projection quantum numbers ($T_3 = 0$ versus $T_3 = 1$) of the nuclear final states the resonances excited in (e, e') and (π^-, γ) reactions decay into different channels characterized by different widths.

In the muon capture reaction most intensively are again excited these 2^- states which form M2 resonance. At the same time the vector current present in the muon capture increases the strength of $J^\pi = 1^-$ states as compared to the (π^-, γ) reaction, and their contribution becomes comparable to that of $J^\pi = 2^-$ states.

The transversal electric dipole (E1t) excitations in the

(e ,e') reactions are mainly connected with the $p_{3/2} \to d_{3/2}$ transition (see table 1), since the dominant is contribution of the $Q_{101}(\nabla/q)$ term of operator (3). The region where E1t transitions are localized lies somewhat higher in energy than that of M2, this is due to the dominant role of the $d_{3/2}$ subshell. The main strength is carried by the 1_5^- level. Similar states show up in the photoabsorption reaction. They form the famous giant dipole resonance. At such a small momentum transfer, however, the 1_4^- level dominates which is built up mainly from $p_{3/2} \to d_{5/2}$ transitions. In the (π^-, γ) reaction the 1^- are excited with lesser intensity as compared with the 180° electron scattering. In the latter case they are enhanced owing to the "orbital" $Q(\nabla/q)$ components of the operator (3).

The strongest peaks resolved [16] in the ^{16}O (π^-, γ) experiment are located near the positions predicted in ref. [14]. In (e ,e') reaction at $E_e = 54.3$ MeV and $\theta = 165°$ the $J^\pi = 2^-$ states are seen [17] at about 20 MeV, too. The excitation is split into two peaks at 19.04 MeV and 20.36 MeV. This is the position where the main M2 strength should appear according to our calculation.

In order to understand the structure of the giant resonance (the M2 component, in particular) and to determine the microscopic structure of the coherent states forming the excitation spectrum of the nuclear system, the nucleon decay channels should be studied. As is known, both the nucleon emission spectra from the decay of resonances to the individual levels of the daughter nuclei (A-1) and the partial excitation spectra for fixed decay channels show resonance structure and reflect the parentage coupling of the giant resonance to the states of daughter nuclei. In this way the particular states forming the resonances can be more clearly selected. For example, observing the ^{16}O $(\pi^-, \gamma n)$ ^{15}N branch one selects the $J^\pi = 2_4^-$ part of the M2 resonance [15] g.s. Indeed, in both the (π^-, γ) and (μ^-, ν_μ) reactions on ^{16}O a salient peak is seen in the neutron spectra at $E_n \approx 4$ MeV, in full agreement with calculation [15]. In the (μ^-, ν_μ) reaction this peak is formed from the $^{16}N(2_4^-) \to {}^{15}N$(g.s.) and $^{16}N(1_5^-) \to {}^{15}N$ ($\frac{3}{2}^-$, 6.32 MeV) branches, each contributing with about equal intensity. For the M2 electroexcitation, the decays to the ground states of ^{15}N and ^{15}O are also expected to dominate.

The experimental data for A=16 system just discussed point

out that in the reactions analysed the M2 resonance states dominate both when the formation of the nuclear excitation and its subsequent decay are considered. It is then important to perform a unified analysis of the above mentioned low-q transfer reactions in other light nuclei as well. In this way we may obtain reasonably complete information about the M2 mode in the nuclear systems.

4. M2 resonance in non-magic N=Z nuclei with $J_{g.s.} \neq 0$. ^{14}N nucleus

Ground state spin of ^{14}N is $J^{\pi}_{g.s.} = 1^+$. The M2 transition is therefore formed from the $1^-, 2^-$, and 3^- nuclear excitations. The contributions of each of these groups are given in table 2.

Table 2. Calculated M2 transitions in the 180° (e,e') scattering and the yield of hard γ-quanta in the (π^-, γ) reaction on ^{14}N.

E^* (^{14}N) (MeV)	J^{π}_f	$\frac{d\sigma}{d\Omega}(M2, T_>)$ (10^{-9} fm^2/sr)	%	R_γ (10^{-4})	%
Strongest individual transitions					
7.0	3^-	62	8	11	6
16.9	2^-	77	10	9	5
17.3	3^-	118	15	12	7
18.1	3^-	77	10	10	5
20.1	2^-	64	8	8	4
20.5	1^-	34	4	-	-
20.7	2^-	20	3	10	5
Sum			58		32
Contributions of all nuclear states with definite J_f					
	3^-	419	55	67	37
	2^-	246	32	64	35
	1^-	100	13	37	20
	$0^-, 4^-, 5^-$	-	-	14	8
Total		765	100	182	100

As for the gross-structure the second and third group dominate. In order to demonstrate the detailed analogy of (e,e') and (π^-,γ) excitation we display in table 2 the strongest individual transitions.

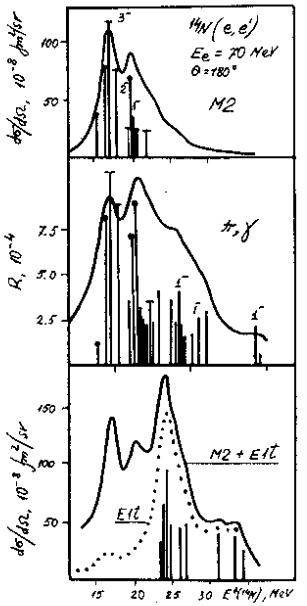

Fig.2. ^{14}N nuclear excitation spectra in reactions (e,e') and (π^-,γ). A Breit-Wigner shape of 2 MeV width was ascribed to each line.

Fig. 2. shows the calculated spectrum of A=14 nuclear excitations. Again, it can be seen that the same transitions build up the M2 resonance in e^- scattering and in the spin-dipole branch of the (π^-,γ) reaction.

Two groups of transitions are distinctly seen both in spectrum of the M2 electroexcitation in ^{14}N and in the ^{14}N (π^-,γ) reaction. The first one is connected with the $J_f^\pi = 2^-$ states and is located at the same position as the M2 resonance in ^{16}O. The second group ($3^-,2^-$) corresponds to somewhat lower excitation energies.

The measured $^{14}N(\pi^-,\gamma)$ yield curve shows signs of the doubly-humped structure predicted earlier [4]. The expected strong 3^- resonance ($E^*(^{14}C)$=6.73 MeV) was, however, not yet confirmed [2,18]. It contrasts with the observation of this 3^- transition in the $^{14}N(\mu^-,\nu_\mu)$ reaction [19].

It was also predicted earlier [4] for the dominating 2^- resonance showing up in $^{14}N(\pi^-,\gamma)$ that it should mainly decay to the lowest $\frac{3}{2}^-$ level in ^{13}C(3.68 MeV) and ^{13}N, the former being accessible to (e,e'pγ) coincidence studies. On the other hand, the higher-lying resonance (3^-1) of the system excited in the $^{14}N(\pi^-,\gamma)$ reaction is expected to feed mainly the $\frac{5}{2}^-$(7.55 MeV) level in ^{13}C. The latter is located above the threshold of subsequent neutron emission. The M2 resonance in (e,e') reaction should decay in the same manner.

E1t transitions form several distinct groups, too. The strongest peak is at the same position as in ^{16}O. Another, less pronounced peak appears at higher nuclear excitation energy and broadens the resonance. It is due to the transitions from the inner 1s-shell ($1s \to 1p_{1/2}$ transition), the latter could not practically be seen in ^{16}O. Therefore, in the case of nonmagic nuclei we observe the so-called configurational splitting of resonance, which is well known [20] from the photonuclear reactions: the coupling between transitions from the unfilled and closed shells is not strong enough to break the isolation of these two groups of transitions. The $1s \to 1p_{1/2}$ core excitations ($E^* \gtrsim 30$ MeV) should contain a larger fraction of the E1 strength than the $1s \to 1p_{3/2}$ excitation in the photo reaction, due to the different p-subshell occupation. As for ^{16}O, the dominant $p_{3/2} \to d_{5/2}$ photo-dipole state ($1^-_4 1$; $E^*=22$ MeV) is only weakly excited at $q \approx m_\pi$. Recent data [21] from ^{14}N (e,e') reaction at $\theta = 180°$ seem to indicate the M2, T=1 strength at $E^* \approx 16.1$ MeV which is consistent with our calculation. The isoscalar M2 and E1t transitions are about one order of magnitude weaker than the isovector ones at the given value of q .

5. Isospin splitting of M2 resonance. Examples of ^{13}C and ^{14}C nuclei

In the photo-dipole excitations, an isospin splitting of the M2 and E1t resonances in $N \neq Z$ nuclei is predicted. Whereas in the photo resonance in 1p-shell nuclei the $T_>$ branch usually dominates, the $T_<$ branches of the M2 resonance at $q \approx m_\pi$ have comparable strength (for the exceptional case ^{14}C and ^{7}Li, see ref.[4]). Figs. 3 and 4 show the isospin branches of the M2 and E1t excitations in ^{13}C and ^{14}C. The M2, $T_>$ resonance ($\Delta J = 2$) is concentrated around $E^*(^{13}C) \approx 21$ MeV and $E^*(^{14}C) \approx 25$ MeV respectively and corresponds again to the dominating (π^-, γ) peaks [$E^*(^{13}B) \approx 5$ MeV and $E^*(^{14}B) \approx 2$ MeV]. The strongest partial transitions and distribution of the strength over the J_f values are given in tables 3-5.

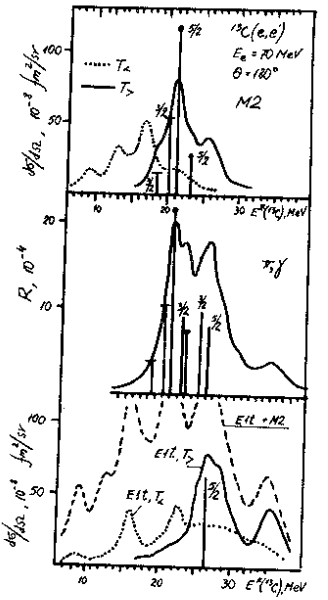

Fig. 3. A=13 nuclear excitation spectra in reactions (e,e') and (π^-,γ).

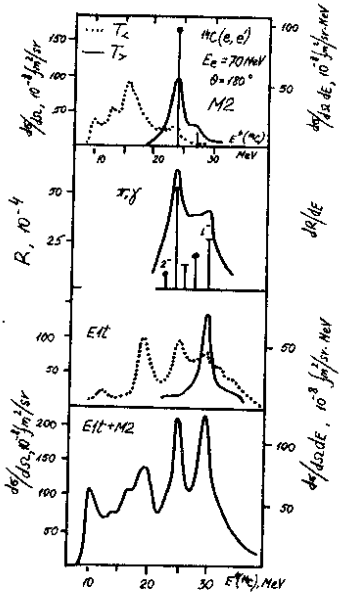

Fig. 4. ^{14}C nuclear excitation spectra in reactions (e,e') and (π^-,γ).

The E1t, $T_>$ resonances are always located at higher energy as compared to the M2, $T_>$. The available evidence for electroexcitation of ^{13}C and ^{14}C in the giant resonance region has already been discussed [12]. The new experimental data on the ^{13}C (π^-,γ) reaction show a nice agreement with our predictions[22]. It supports the reliability of our analysis of the M2 strength in the A=13 system.

Table 3.

The same as in table 2, except for ^{13}C

$E^*(^{13}C)$ (MeV)	J_f^π	$\frac{d\sigma}{d\Omega}(M2, T_>)$ (10^{-8} fm^2/sr)	%	R_γ (10^{-4})	%	$\frac{d\sigma}{d\Omega}(M2, T_<)$ (10^{-8} fm^2/sr)	%
Strongest individual $T_>$ transitions							
18.2	$5/2^+$	24	6	-	-		
18.5	$3/2^+$	21	6	12	8		
20.1	$3/2^+$	52	14	10	7		
21.1	$5/2^+$	118	31	24	16		
23.1	$5/2^+$	26	7	8	5		
25.2	$3/2^+$	33	9	11	7		
26.3	$5/2^+$	27	7	9	6		
Sum			80		49		
Contributions of all nuclear states with definite J_f							
	$3/2^+$	I45	38	66	43	I06	32
	$5/2^+$	232	62	57	37	223	68
		-	-	30	20	-	-
Total		377	I00	I53	I00	329	I00

Table 4.

Total cross section (10^{-8} fm^2/sr) of inelastic electron scattering at $\theta = 180°$ in ^{14}C and yield of γ-quanta in ^{14}C (π^-, γ) reaction

	$T_<$	$T_>$
E1t	689	290
M2	502	267
(π^-, γ)	-	150

Table 5.

The strongest transitions, which form M2-resonance in ^{14}C

$E^*(^{12}C)$	$\frac{d\sigma}{d\Omega}(M2,T_>)$		P_γ
(MeV)	(10^{-8}fm^2/sr)	%	(10^{-4})
22.8	40	15	9
24.2	170	64	53
27.4	30	11	19
		90	

6. Configurational splitting of the M2 resonance. Examples of ^{7}Li.

For the lightest 1p-shell nuclei (A=6,7) a considerable configurational splitting of the M2 resonance is expected between transitions 1p→1d , 2s and 1s→1p, similarly as is indicated in the ^{6}Li (π^-,γ) and ^{7}Li photo excitations. Both groups (see table 6) of transitions in ^{7}Li should have about the same strength due to the shell occupation. Because of the important contributions from the core excitations ($E^* \gtrsim 30$ MeV), the M2 resonance is shifted towards rather higher energies than for the heavier 1p-shell nuclei, cf. figs. 1 and 2. As a result we can see, that two factors actually determine the gross structure of the M2 and E1t resonance in ^{7}Li, namely the isospin (see fig. 5) and the configurational (see fig.6) splitting. Again, the $T_>$ branch of the M2 electroexcitation is connected with the same transitions which build up the main maximum in the (π^-,γ) reaction.

Table 6.

The same as in table 2 except for ^{7}Li

E^* (^{7}Li) (MeV)	J_f^π	$\frac{d\sigma}{d\Omega}(M2,T_>)$ (10^{-8} fm^2/sr)	%	R_γ (10^{-4})	%	$\frac{d\sigma}{d\Omega}(M2,T_<)$ (10^{-8} fm^2/sr)	%
Strongest individual $T_>$ transitions							
14.8	$1/2^+$	20	12	12	6		
16.7	$5/2^+$	46	27	36	17		
26.8	$3/2^+$	18	11	15	7		
31.4	$5/2^+$	28	16	30	14		
32.7	$7/2^+$	14	9	12	6		
Sum			75		50		
Contributions of all nuclear states with definite J_f							
	$1/2^+$	30	18	33	16	33	17
	$3/2^+$	35	21	61	31	21	12
	$5/2^+$	86	51	89	45	79	42
	$7/2^+$	18	10	15	8	55	29
Total		169	100	198	100	188	100

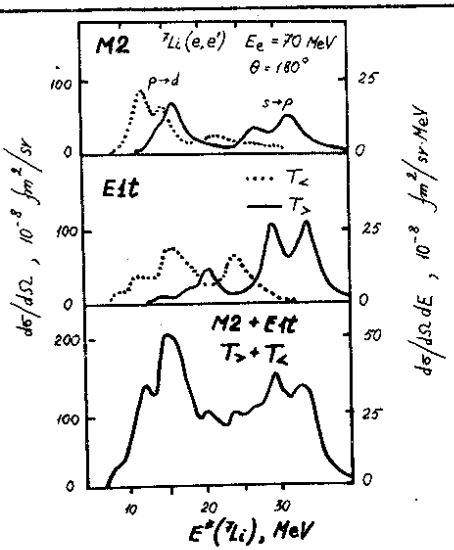

Fig. 5. The isospin splitting of M2 and E1t resonances in ^{7}Li.

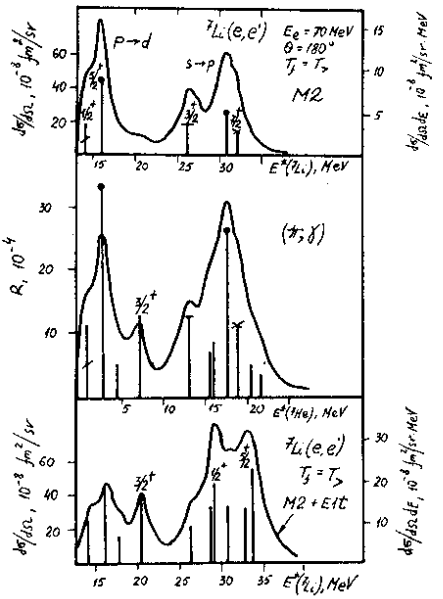

Fig. 6. A=7 nuclear excitation spectra in reactions (e,e') and (π^-, γ).

7. Nuclei with half-filled 1p-shell.
Example of ^{9}Be.

With the increasing 1p-shell occupation the role of the 1s excitations and, hence, the configurational splitting of the multipole resonances must die off and the mean resonance energy therefore decreases; here we have a full analogy with the photo resonance. The M2 resonance in ^{9}Be is already dominated by the $p_{3/2} \rightarrow d_{5/2}$ valence excitation. An analogous shift of the main peak is observed in the (π^-,γ) reaction [2]. The E1t resonance, however, is still at energies above 30 MeV since it still contains considerable contributions from the 1s core excitation. Table 7 and fig. 7 show the strongest partial transitions forming the M2, $T_>$ resonance in ^{9}Be and the distribution of the transition strength over the final state spins. The same conclusions are valid for the A=11 nuclei.

Table 7.

The same as in table 2 except for ^{9}Be.

E^* (^{9}Be) (MeV)	J_f^π	$\frac{d\sigma}{d\Omega}$ (M2, $T_>$) (10^{-8} fm^2/sr)	%	R_γ (10^{-4})	%
Strongest individual transitions					
18.1	$3/2^+$	6	3	2	2
19.0	$5/2^+$	19	9	6	5
19.1	$3/2^+$	5	3	4	3
20.4	$7/2^+$	35	16	9	7
20.9	$5/2^+$	16	7	5	4
21.8	$7/2^+$	21	10	7	6
27.1	$1/2^+$	14	6	5	4
Sum			54		31
Contributions of all nuclear states with definite J_f					
	$1/2^+$	37	17	22	18
	$3/2^+$	38	18	28	24
	$5/2^+$	70	32	47	39
	$7/2^+$	72	33	22	19
Total		217	100	119	100

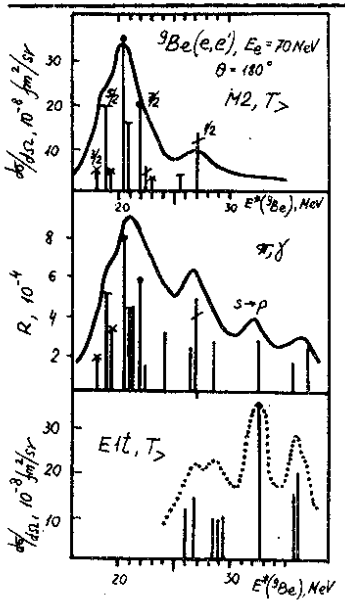

Fig. 7. A=9 nuclear excitation spectra in reactions (e,e') and (π^-,γ).

8. M2 resonance beyond the 1p shell

The dominant role of M2 excitations in the (π^-,γ) reactions weakens already for the 2s, 1d-shell nuclei (see,e.g.,[23]). The pions are captured from mesoatomic orbitals with larger momenta (ℓ_π =2,3) and give rise to higher nuclear multipolarities. Nevertheless, one expects that the pion capture in flight as well as the electro- and photo-production reactions should be again dominated by the low-spin transitions. By now data are already available showing the effects of giant resonance excitations in the $(e,e'\pi)$ reaction [24] on the 1p-shell nuclei. The role of the giant resonances is analogous to that in the (π^-,γ) process at rest. An extension of such experimental and theoretical studies should help one to complete the systematics and to understand the specific features of the M2 mode in heavier nuclei. In particular the $T_>$ branch of the giant resonances is suppressed in the photo- and low-q electro-excitations on heavier nuclei. The (γ,π) and $(e,e'\pi)$ processes can open the selective channels of their study.

9. Conclusions

1. The analysis performed predicts that the M2, $T_>$ branch of the giant resonance excited in the low-q backward electron scattering, the ΔJ =2 branch in the muon capture, and the main resonance in the radiative pion capture on the 1p-shell nuclei are all built out of the same transitions. It follows then that the presently available (π^-,γ) data should provide clear evidence on the localization and the gross structure of the M2, $T_>$ resonance showing up in the backward electron scattering.

2. As a result of the shell-model analysis, the following main features of the M2 resonance are expected:

(i) At the upper end of the 1p-shell the M2 resonance is mainly formed by the $1p_{3/2} \longrightarrow 1d_{5/2}$ transitions and is located at $E^* \approx 16 \div 20$ MeV. (The other M2 peaks show rather lesser intensity). In the lightest 1p-shell nuclei (^{6,7}Li) the 1s core excitations and valence excitations contribute comparably to the cross section, this results in a configurational splitting of the M2 resonance, a considerable part of M2 strength is therefore shifted towards higher energies. With the increasing occupation of the 1p shell the contributions from core excitations to the M2 resonance decrease.

(ii) In nuclei with N≠Z the M2 resonance will be isospin-split with $T_>$ branch shifted to higher E^*. The relative strength of both the isospin branches (at $q \approx m_\pi$) is on the average equal, exceptions being due to the specific structure of the target ground state (^{7}Li, ^{14}C).

3. The transversal E1 excitations are connected with the spin-flip $1p_{3/2} \longrightarrow 1d_{3/2}$ transitions and therefore are located at higher excitation energies than the M2 resonance.

4. The direct tests of the predictions concerning the structure of the M2 resonance in the light nuclei should be performed in the inelastic 180° electron scattering experiments and, on a complementarity basis in the studies of the selective decay channels of the giant resonances excited in the (π^-, γ) reaction.

5. Though experimentally more difficult, the pion photo- and electro-production on nuclei are expected to open new possibilities for studying the low-multipole magnetic modes.

References

1) H.W.Baer, K.M.Crowe, P.Trüol, Advances in Nuclear Physics, vol.9, ed.M.Baranger and E.Vogt (Plenum Press, N.Y., 1977), p. 177.
2) J.P.Perroud, Photopion Nuclear Physics, ed. P.Stoler (Plenum Press, N.Y., 1979), p. 69.
3) H.R.Kissener, G.E.Dogotar, R.A.Eramzhyan and R.A.Sakaev, Nucl.Phys. A302 (1978) 523.
4) H.R.Kissener, G.E.Dogotar, R.A.Eramzhyan and R.A.Sakaev, Nucl.Phys. A312 (1978) 394.
5) A.Richter, in Proc. 4th Seminar Electromagnetic Interactions of Nuclei at Low and Intermediate Energies (Nauka, Moscow, 1979).
6) J.Speth, In Proc. Int. Conf. on Nuclear Physics with Electromagnetic Interactions, Mainz 1979.
7) W.Knüpfer, R.Frey, A.Friebel, W.Mether, D.Mener, A.Richter, E.Spamer and O.Titze. Preprint Darmstadt IKDA 78/9; Phys.Lett. 77B (1978) 367.
8) S.S.Hanna, SLAC preprint 1979.
9) V.O.Nesterenko, JINR P4-12513, Dubna, 1979.
10) V.Yu.Ponomarev, V.G.Soloviev, Ch.Stoyanov and A.I.Vdovin, Nucl.Phys. in print.

11) J.S.Dehesa, Dissertation, Jülich, Jul - 1425, 1977.
12) H.R.Kissener and R.A.Eramzhyan, Nucl.Phys. in print; in Photopion Nuclear Physics, ed. P.Stoler (Plenum Press, N.Y., 1979) p. 117.
13) G.E.Dogotar, R.A.Eramzhyan, H.R.Kissener and R.A.Sakaev, Nucl.Phys. A282 (1977) 474.
14) R.A.Eramzhyan, M.Gmitro, L.A.Tosunjan and R.A.Sakaev, Nucl.Phys. A290 (1977) 294.
15) R.A.Eramzhyan, M.Gmitro and L.A.Tosunjan, J.Phys.G: Nuclear Physics 4 (1978) L233; Czech.J.Phys. B29 (1979) 370.
16) G.Strassner et al. Phys.Rev. in print.
17) A.Goldmann and M.Stroetzel, Z.Phys. 239 (1970) 235.
18) J.C.Alder et al., in Photopion Nuclear Physics, ed. P.Stoler (Plenum Press, N.Y., 1979) p. 101.
19) E.Bellotti, W.Dey, R.Engfer, E.Fiorini, P.Negri, H.J.Pfeiffer and H.K.Walter, SIN Physics Report no. 1, (Dec.1976) p. 41.
20) V.G.Neudachin, in Proc. Int. Conf. on Electromagnetic Interactions at Low and Intermediate Energies. Vol. 3, (Moscow, 1967) p. 351.
21) N.Ensslin, L.W.Fagg, R.A.Lindgren, W.L.Bendel and E.C.Jones, Jr., Phys.Rev. C19 (1979) 569.
22) P.Trüol, in Proc. Int. Conf. on Nuclear Physics with Electromagnetic Interactions, Mainz, 1979.
23) R.A.Eramzhyan, L.Majling, J.Řízek and R.A.Sakaev, Czech. J. Phys. B28 (1978) 1081.
24) K.Shoda, M.Yamazaki, K.Nakahara and H.Ohashi, in Photopion Nuclear Physics, ed. P.Stoler (Plenum Press, N.Y., 1979) p.205.

Received by Publishing Department
on July 23 1979.